MANGROVE FOREST DISTRIBUTION AND DYAMICS OF THE CA MAU PENINSULA, MEKONG DELTA USING LANDSAT IMAGERY

Tran Thanh Dan[1,2] and Susumu Ogawa[2]
[1]Department of Land Resources, College of the Environment and Natural Resources, Can Tho University, Viet Nam
Email: ttdan@ctu.edu.vn
[2]Department of Science and Technology, Graduate school of Engineering, Nagasaki University, Japan
Email: ogawa_susumu_phd@yahoo.co.jp

KEY WORDS: Coastline erosion, Data preprocessing, Landsat, Mekong Delta, Mangrove forest

ABSTRACT: In the past three decades, land covers have changed in the Mekong delta, Vietnam with difficulty for stable and sustainable management. Therein, mangrove has significantly changed during that period due to shrimp culture development rapidly. Therefore, monitoring a spatio-temporal distribution and changes of mangrove is critical for natural resource management. To contribute better management for mangrove and coastlines in the area, the research objectives were: to map the current extent of mangrove in Camau peninsula from 1989 to 2015, and to identify change of mangrove. The data were processed through four main steps: (1) data pre-processing including atmospheric correction, image normalization, and cloud removal, (2) image classification using supervised classification approach, (3) accuracy assessment, and (4) change detection analysis. Validation was made by comparing the classification result with the ground reference data, which yielded agreement with overall accuracy 77.4% and Kappa coefficient of 0.68. The results showed that mangrove has decreased by half (236.07 km2) from 1989 to 1998 due to shrimp culture. At the same time, the area of mix shrimp and mangrove increased by 386.69 km2 (about 88%). However, mangrove and mix mangrove, and shrimp areas have been raised by twice for mangrove and about 11% for mix mangrove and shrimp, respectively, in the second period from 1998 to 2015. These changes of mangrove were affected by two activities: deforestation, and replanting or newly formed. The development of aquaculture has been increasing quite rapidly and in an unplanned way. It also caused environmental and natural resources problem as well as socio-economic aspects. Research results for mangrove mapping and change detection in the study area are capable of providing quantitative information of long-term land-use change for coastal management in the Mekong delta.

1. INTRODUCTION

Mangrove grows in river deltas, estuarine complexes and coasts in the tropical and subtropical regions throughout the world. The total mangrove area accounts for 0.7% of total tropical forests of the world. The largest extent of mangrove is found in Asia (42.0%) followed to Africa (20.0%), North and Central America (15.0%), Oceania (12.0%) and South America (11.0%) (Giri et al., 2011). Therein, Vietnam is estimated to have 1580 km2 of mangrove ranking 24 among 118 countries and territories supporting mangrove. It is estimated that the area of mangrove was about 4,000 km2 in the 1940s. However, this area has declined dramatically, especially since the 1980s. Much of this loss can be attributed to the conversion of forests into rice fields and, more recently, shrimp ponds (loss of approximately 76.4% of mangrove according to Spalding et al., 2010). Therein, mangrove in the Mekong Delta was covered more than 250,000 ha (Maurand, 1943 cited in Hong and San, 1993) and mainly distributed in Camau peninsula (CMP). In the past three decades, mangrove was reduced due to deforestation for fuel, wood construction, the war, forest fire and other human activities. Especially, mangrove forests have been cleared for shrimp farming in many areas with thousands hectare of mangrove (Hong and San, 1993; Hong, 1995; and Hao, 1999) since the end of 1980s and in the 1990s. It is consumed that there were many factors that have affected the mangrove changes of the delta, and the most important factor that was the shrimp culture activities with the high economic returns, resulted of mangrove restructure. The pattern of land uses in the Mekong Delta has been changed significantly over decades.

The availability of the earth observation satellite data like Landsat data is useful for change detection applications. The distribution and abundance of mangrove in different regions of the world have been assessed with a variety of techniques. Based on the importance and vulnerable of mangrove ecosystems faced, many studies on mangrove have been conducted to solve these issues in different scales, long-term monitoring and detecting mangrove by using remote sensing techniques (Blasco et al., 2001; Everitt et al., 2008; Giri et al., 2007; Green, 1998; Seto and Fragkias., 2007; and Vaiphasa et al., 2006). In addition, change detection is a powerful tool to visualize, to measure, and better to understand a trend in mangrove ecosystems. It enables the evaluation changes over a long period of time as well as the identification of sudden changes due to natural or dramatic anthropogenic impacts (e.g. tsunami destruction or conversion to shrimp farms). Thus, distribution, condition, and increase or decrease were the measured features used in the change-detection applications of mangrove. Monitoring change in mangrove was adopted by many researchers throughout the world (Giri et al., 2011; Giri et al., 2007; Ruiz and Berlanga, 2002; Concheddaa et al., 2008; Selvam et al., 2003; Chen et al., 2013), and the applications of the supervised classification approaches were the most effective and robust method for classifying mangrove based on traditional satellite remote sensing data. Thus, our objective was monitoring and detecting changes in mangrove in the Mekong Delta under these conditions. For this reason, the research was adopted to detect spatial and temporal change in mangrove during the past decades, from 1989 to 2015 by using Landsat satellite data with a supervised classification approach. Hence, the results provided important information for the local government to make a decision for better land use planning and land management in the future.

2. MATERIALS AND METHODS

2.1 Study area

The study area is located at the southernmost of Ca Mau province in the Mekong Delta, between latitude 8032’–8049’ N and longitude 104040’– 105019’ E (Fig. 1). It covers Ngoc Hien district and partly Cai Nuoc and Dam Doi districts. CMP was originally the largest area and best developed mangrove in Vietnam (Hong and San., 1993). Due to economic development driven by societal needs, the region experienced a significant conversion of mangrove to aquaculture, especially shrimp farms. Approximately, 77389 ha of mangrove in this region was converted to aquaculture systems, during 1983–1995 (Jacques et al., 2002), making this province the largest shrimp exporter in the country (GSO, 2012). Although shrimp farming brought benefits to the region, the rapid conversion of mangrove ecosystems to shrimp farms without a proper land-use planning has caused environmental impacts, including coastline erosion and loss of habitats and breeding grounds of aquatic species (VNEPA, 2005).

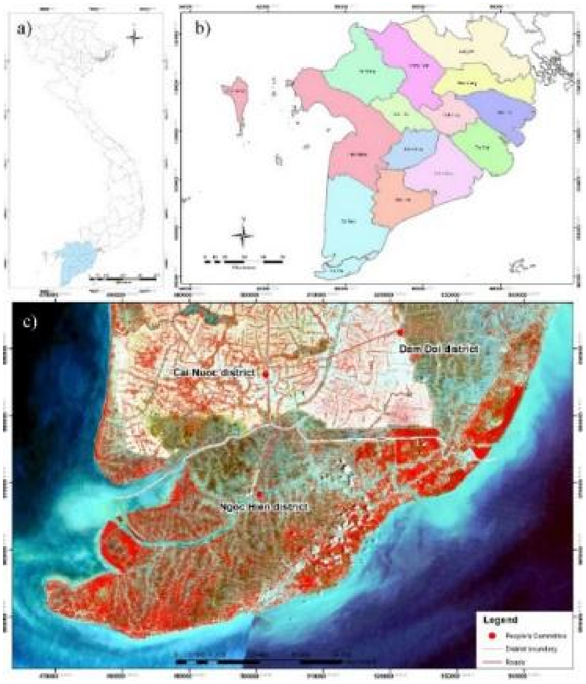

Fig. 1. Study area. a) Vietnam map, b) Mekong delta Administrative map, and c) Landsat data in 1998 after pre-processing.

2.2 Data collection

A series of Landsat imageries in 1989, 1998, and 2015 were collected from the USGS via the website, http://earthexplorer.usgs.gov/. Images acquisition dates are very important because vegetation and crops reflect differently at the beginning and the end of the rainy season due to phenological and temperatures disparities, and their reflectance varies from the dry season to the rainy season. Therefore, satellite data were collected in the same dry season during three periods. The Landsat TM and ETM+ have 7 spectral bands with a spatial resolution of 30 m for bands 1-5 and 7. The TM and ETM+ band 6 (thermal infrared) is acquired at 120 m and 60 m resolution but are resampled to 30 m pixels, respectively. The Landsat 8 data have 9 spectral bands with a spatial resolution of 30 m for bands 1-7 and 9, while band 8 has a spatial resolution of 15 m (panchromatic band). The level 1T provides systematic radiometric and geometric accuracy by incorporating ground control points while employing a Digital Elevation

Model (DEM) for topographic accuracy and were projected to World Geodetic System 1984 (WGS84) Universal Transverse Mercator (UTM).
The land use map in the study area in 2014 was collected from the Department of Land Resources, Can Tho University, Vietnam for validating interpreted mangrove maps. In addition, this research used Google Earth and other reference maps (administrative maps, land cover maps which interpreted from satellite imagery), reports and literatures on the states of the mangrove distribution for additional information in the study area.

Table 1. Bands line up, wavelengths, and description of each Landsat band

Band name	Wavelength (µm)		Useful for mapping
	Landsat TM/ ETM+	Landsat 8 OLI	
Coastal	-	0.43 – 0.45	Coastal and aerosol studies
Blue	0.45 - 0.52	0.45 – 0.51	Bathymetric mapping, distinguishing soil from vegetation and deciduous from coniferous vegetation
Green	0.52 - 0.60	0.53 – 0.59	Emphasizes peak vegetation which is useful for assessing plant vigor
Red	0.63 - 0.69	0.64 – 0.67	Discriminates vegetation slopes
NIR	0.76 - 0.90	0.85 – 0.88	Emphasizes biomass content and shorelines
SWIR 1	1.55 - 1.75	1.57 – 1.65	Discriminates moisture content of soil and vegetation; penetrates thin clouds
SWIR 2	2.08 - 2.35	2.11 – 2.29	Improved moisture content of soil and vegetation and thin cloud penetration
Pan	0.52 - 0.90	0.50 – 0.68	15 meter resolution, sharper image definition
Cirrus	-	1.36 – 1.38	Improved detection of cirrus cloud contamination
TIRS 1	10.4 - 12.50	10.6 – 11.19	100 meter resolution, thermal mapping and estimated soil moisture
TIRS 2	-	11.5 – 12.51	100 meter resolution, thermal mapping and estimated soil moisture

2.3 Methods

2.3.1 Image pre-processing

This research used all spectral bands and NDVI (an additional band) to perform image classification. Because remotely sensed data acquired showed some forms of distortion or shift in geometric location from one sensor to the other. Therefore, image registration was necessary to fix this problem. Ground control points were used to correct geometric and a root mean square error (RMSE) of 0.58, 0.63, and 0.51 pixels in 1989, 1998, and 2015, respectively, were obtained in the study area. Landsat TM and ETM+ used in Climate Data Records (CDR) products. The surface reflectance CDR generated from specialized software called Landsat Ecosystem Disturbance Adaptive Processing System (LEDAPS). The software applies MODIS atmospheric correction routines to Level-1 Landsat TM or ETM+ data. Water vapor, ozone, geopotential height, aerosol optical thickness, and digital elevation were input with Landsat data to the Second Simulation of a Satellite Signal in the Solar Spectrum (6S) radiative transfer models to generate the top of atmosphere (TOA) reflectance, surface reflectance, brightness temperature, and to mask clouds, cloud shadows, adjacent clouds, land, and water. In this case, the atmospheric correction only performed for Landsat 8 using Actor 2 (flat terrain, two geometric degrees-of-freedom (DOF)) software. The detailed parameters applied for the atmospheric correction presented in Table 2.

Table 2. Parameters used for atmospheric correction model.

Sensor	Landsat 8 OLI	
Date	2015/01/15	2015/02/27
Solar zenith angle (deg)	35.5	34.9
Solar azimuth angle (deg)	123.3	135.3
Water vapor category	Tropical	Tropical
Aerosol type	Maritime	Maritime
Average visibility (km)	39	39

As the results of images acquisition, the dates determined the image quality. Satellite data had different imageries on different dates in one period. Thus, reflectance normalization was performed with a histogram matching model and was developed within Imagine. It was identical to histogram matching based on equating cumulative distribution functions. However, it used only image overlap areas to determine a lookup table for matching. This research was developed a model to match these images, called Histogram Matching Model (Fig. 2.). The goal was to generate satellite-image mosaics that are amenable to classification methods.

Furthermore, the site of study was a big size. Hence, the subset study area was reduced from the bulk, and the size of information was processed. This reduced the time consumed for the analysis of satellite images and also speeded up processing due to small amount of data processed. Besides, this area was covered by clouds during whole year. Hence, cloud removal was necessary to generate cloud free data for image classification. The NSPI approach used a weighted linear model to predict spectral values of a target pixel from its neighboring similar pixels (Chen et al., 2011). Following idea of NSPI, neighboring pixels around cloudy pixels had a similar change trend of reflectance to cloudy pixels if their spectral characteristics were similar. Thus, it was possible to employ a modified NSPI approach to restore spectral values of cloudy pixels using the information of the neighboring similar pixels. For more details, see Chen et al., 2011.

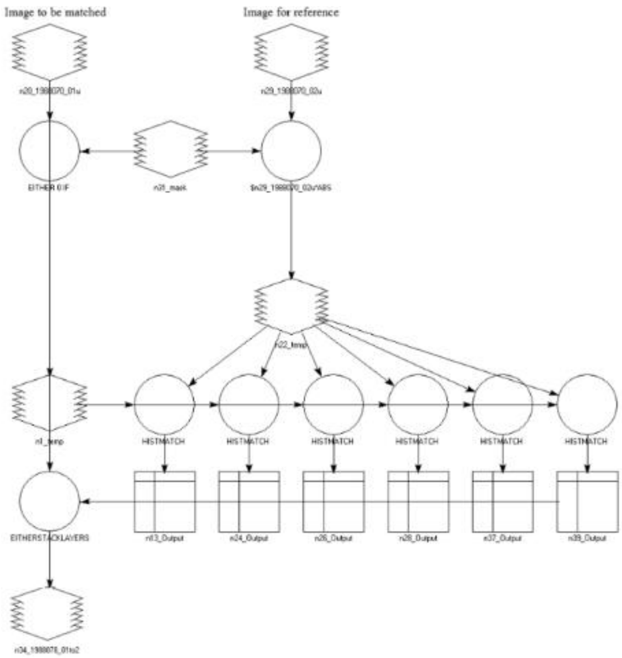

Fig. 2. Histogram matching model was built by using ERDAS software.

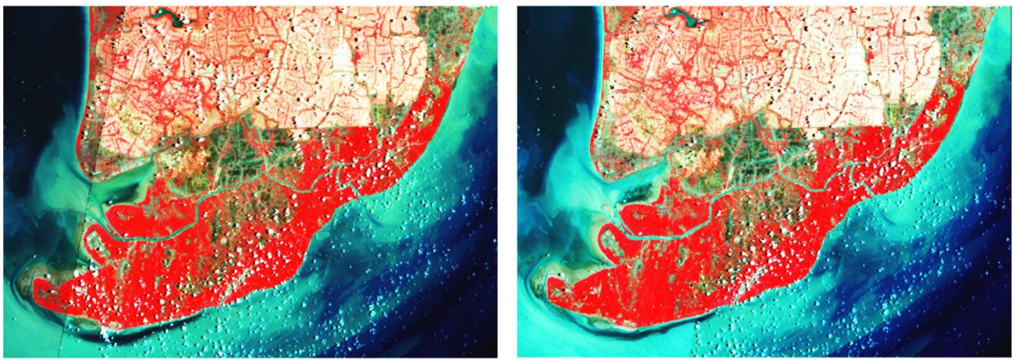

Fig. 3. Results after image normalization and cloud removal.

2.3.2 Image classification

Selection and evaluation training samples

From the training samples, examples of land cover types of interest was identified on the image. The image processing software system was then used to develop a statistical characterization of the reflectance each class. The image was classified by examining the reflectance each pixel and made a decision for which of the signatures it resembled the most (Eastman, 1995). For each study period, the Region of Interest (ROI) tool that provided in ENVI was used to select the training samples. Totally, there were eleven ROIs selected, including mangrove, mix shrimp and mangrove, shrimp, cultivation, built-up, perennial plant, other plants, sediment, water, cloud, and shadows. Each

ROI represented a land cover category. Then, they was evaluated.

A separability test is one of methods to determine how similar the distributions for two groups of pixels are. The Jefferies-Matusita (JM) distance was a function of separability that directly related to the probability of how good a resultant classification will be (Swain et al., 1971). As the results of training data selection, it were evaluated for agreement to classify the images by using the JM from the following form:

$$BD = \frac{1}{8}\,[\mu_i - \mu_j]^T \left(\frac{\epsilon_i - \epsilon_j}{2}\right)^{-1} [\mu_i - \mu_j] + \frac{1}{2} \ln\left[\frac{\frac{1}{2}|\epsilon_i + \epsilon_j|}{\sqrt{|\epsilon_i||\epsilon_j|}}\right] \tag{1}$$

In which β_{ij} is the Bhattacharya Distance and is given by

$$J_{ij} = \sqrt{2(1 - e^{-\beta_{ij}})} \tag{2}$$

where i and j are the two signatures classes, μ_i is the mean vector signature for class i , ϵ_i is corresponding class covariance matrix signature, T is the transposition function. The JM distance had values 0 to 2. If JM value was greater than 1.9, then the classes show good separability. If the value was between 1.7 - 1.9, the separation between the classes was fairly good below 1.7, and the classes were poorly separated (Jensen, 1996).

Image classification

The Support Vector Machine (SVM) algorithm was a non-parametric classifier. The method based on statistical learning theory using a kernel function to non-linearly project the training data in the input space into a higher dimensional space, where the classes were linearly separable. The SVM has been widely applied in remote sensing for classification of land uses or land cover types. It has been demonstrated to give better classification results among the maximum likelihood, univariate decision trees, and back-propagation neural networks (Huang et al., 2002). Nevertheless, it was also claimed that using the SVM for classifying high-dimensional datasets can produce more accurate results comparing with the traditional classifiers, but the outcome greatly depends on the kernel types used, the choice of parameters for the chosen kernel and the method used to generate the SVM.

However, because classified images often manifested a salt-and-pepper appearance due to the inherent spectral variability encountered by a classification when applied on a pixel-by-pixel basis. Therefore, it was desirable to "smooth" or "filter" the classified output. The median filtering in Convolution and Morphology tools in ENVI was used for post classification filtering by using a kernel size of 3x3. The median filtering to smooth an image, while preserving edges larger than the kernel dimensions in removing salt and pepper noise or speckle by replacing each center pixel with the median value within the neighborhood specified by the filter size (Castro and Donoho, 2009).

Accuracy assessment

The accuracy check was done by comparing the classification result with reference data that were believed to reflect the true land cover accurately. In this work, user's, producer's, and overall accuracies together with kappa statistics were derived from the error matrix. The producer's accuracy referred the fraction of correctly classified pixels with regards to all pixels of that ground truth class. The user's accuracy, referred to the reliability of classes in classified images. The kappa statistic incorporated the diagonal elements of the classification error matrix, and represented agreement obtained after the elimination of the proportion of agreement that could have occurred by chance. According to Landis and Koch (1977), Kappa values were grouped into several categories. Values less than zero (0) indicated no agreement, 0-0.2 was regarded as slight agreement, 0.21-0.40 were considered fair, 0.41-0.60 were considered moderate, 0.61-0.80 were substantial, and 0.81-1 represented an almost perfect agreement.

2.3.3 Change detection

The post-classification change detection algorithm was used to determine the change in mangrove from the three different classified images. It was comprised of comparative analysis of independently produced classification maps on different dates, via a mathematical combination of pixel by pixel. The output of this algorithm was in the form of a matrix showing the initial parameter values of different land covers on the columns, and their final state parameters along the rows, together with their respective spatial representation images. The procedure was carried out at two different intervals, for example, the change that occurred during 1989-1998, 1998-2015, and finally from 1989 to 2015. This was perhaps the most common approach to change detection (Jensen, 1996). It was successfully used by many researchers.

3. RESULTS

The analyzing results of land use distribution which interpreted from Landsat data in 1989, 1998, and 2015 are presented in Fig. 4. The classification results presented 11 major classes mapped, including mangrove forests, mix mangrove forests and shrimp, shrimp pound, agriculture, water bodies, sediment, mix built up area and perennials, other trees, cloud and shadow. The results showed that land covers have changed significantly in the study area by visual. Most of land conservation was mangrove and agriculture. For validation of the classification result, the ground reference map in 2014 was converted from vector data to raster data by using Polygon to Raster (with 30m resolution) function in ArcGIS. Then, a 100 random points was created for each class to validate a classification result. The accuracy check was agreed when compared with classification results and the ground truth data with overall accuracy was 77.4% and kappa coefficient was 0.68 in 2015.

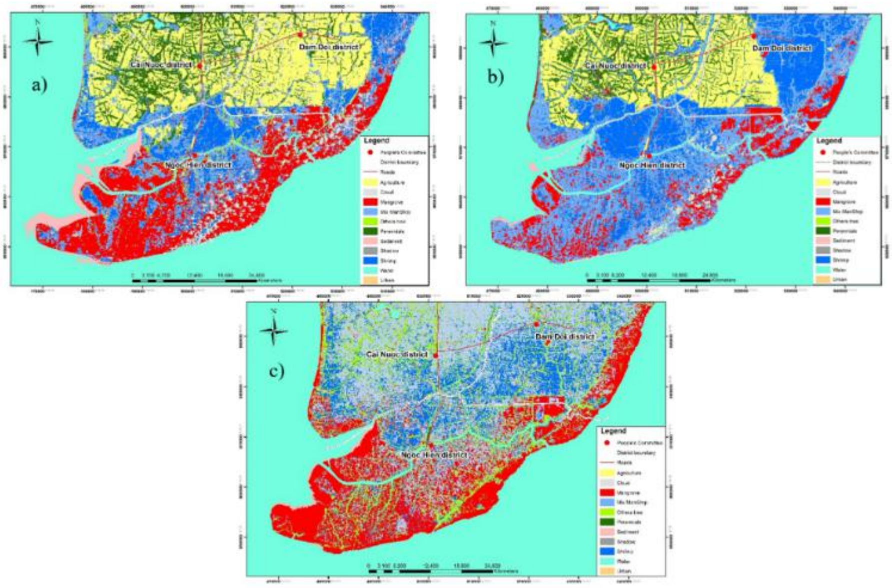

Fig. 4. Classification results in a) 1989, b) 1998, and c) 2015.

3.1 Spatial distribution of mangrove

Spatiotemporal distribution of mangrove showed for three particular years of 1989, 1998 and 2015 in Fig. 5.

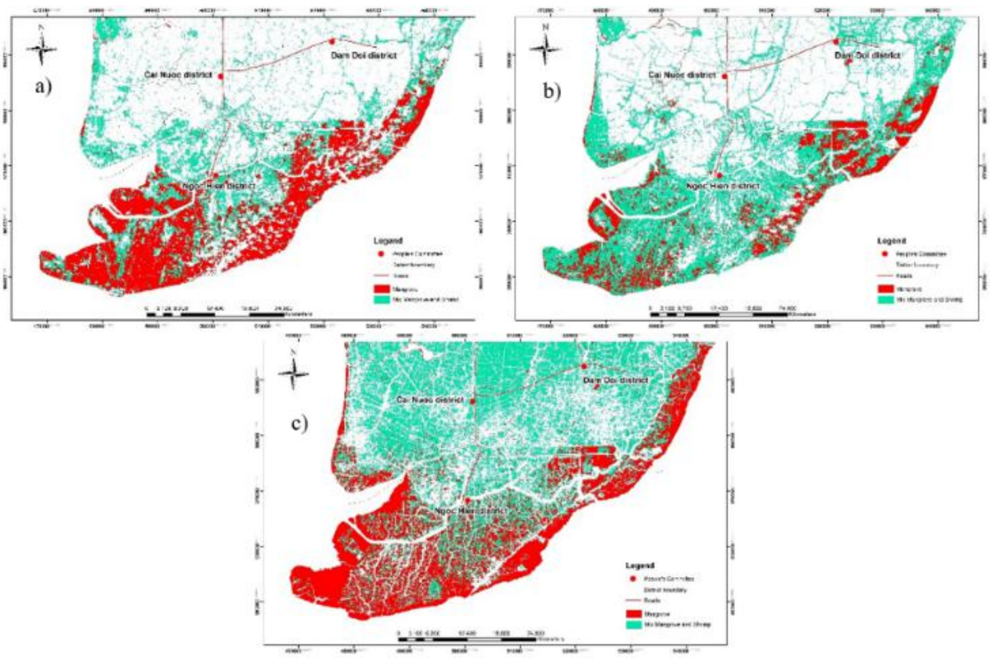

Fig. 5. Spatial distribution of mangrove forests derived from Landsat imagery in a) 1988, b) 2001, and c) 2014.

Mangrove in the area was concentrated in the coastal estuaries, and rivers where interlinked between land and the sea. The main concentration was located in Ngoc Hien district with high dense of mangrove. The result of classified maps in 1989, 1998, and 2015 showed that the total mangrove areas were 519.12 km2 (20.85%), 283.05 km2 (11.68%), and 630.03 km2 (26.37%), while the mix mangrove and shrimp area were 425.84 km2 (17.10%), 802.53 km2 (33.13%), and 897.34 km2 (37.56%), respectively (Fig. 6). This area was strictly managed by the local governments as natural reserves for biodiversity conservation. Mangrove in the upper part was relatively fragmented due to the development of shrimp culture. The study area showed significant rates of mangrove loss in the upper part of the CMP, largely due to conversion to agriculture.

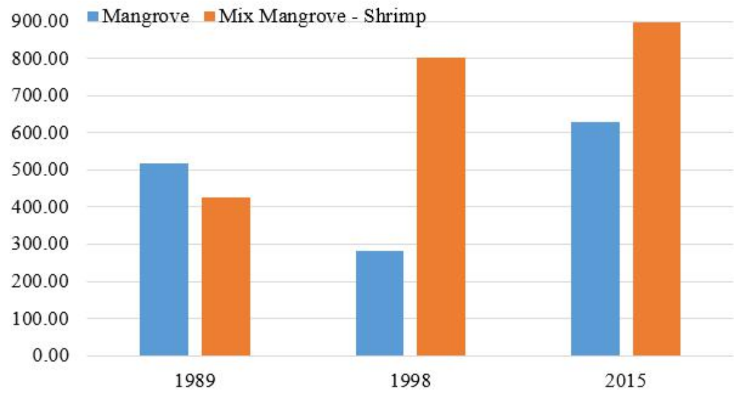

Fig. 6. Real estimation of mangrove and mix mangrove and shrimp during the past three decades.

3.2 Mangrove change detection

Changes in mangrove in difference periods were analyzed and are shown in Fig. 7 and Table 3. The mangrove cover in CMP has significantly changed during the past three decades. Mangrove has been reduced rapidly due to shrimp culture and deforestation for wood construction and fuel. From 1943 to 1993, mangrove was destroyed by the war and other human activities such as cutting down for firewood and converting to paddy fields (Hong and San, 1993), but from 1998 to 2015 reduction of mangrove was contributed by shrimp farm activities. In the results, most land use was covered to mix mangrove and shrimp culture as well as aquaculture. Mangrove has been subjected to enormous pressures and threats within past three decades. The loss of mangrove from 1989 to 2015 was approximately 230.7km2 (9.5% of the total area) (therein, converted to mix mangrove and shrimp was 3.7%), while 11.3% (277.4km2) was recovered or newly planted at the same time. The conversion of the other land uses to mix mangrove and shrimp significantly increased by 25.4% of the total area (619.6km2) (Table 3).

Table 3. Change in mangrove from 1989 to 2015

1989	2015					
	Mangrove		Mix Mangrove-Shrimp		Others	
	km^2	%	km^2	%	km^2	%
Mangrove	288.6	11.8	89.7	3.7	140.8	5.8
Mix Mangrove-Shrimp	125.1	5.1	129.0	5.3	171.7	7.0
Others	152.3	6.2	619.6	25.4	722.9	29.6

Although reforestation areas were 11.3% (therein mangrove had newly formed from sediment area about 6%) of the total mangrove areas, they demonstrated strategies of reforestation were noted in CMP before 2000. As a result, the area of mangrove in the study has only 283.05 km2 in 1998 and covered 11.68% of the total land area. Although there are factors affecting the analysis of remote sensing image results in identification of mangrove, such as images covered by cloud and data outside image area of mangrove in 1998 could be higher than 283.05 km2. In addition, together with results of data analysis, a part of mangrove areas with low density were areas of mixing between mangrove with shrimp culture or mangrove with canal.

Further, changes of mangrove came from not only deforestation but also from replanting in some areas. These two activities, including deforestation and reforestation, occurred seemingly at the same time. Therefore, in 1998 – 2015 period, replanting activities and new formed mangrove were noted and improved more than before the period. In addition, some areas of mangrove were unchanged but their quality was changed (density of mangrove). Most these unchanged areas were located in conversation parts or mangrove biosphere areas such as Dat Mui and Cham Chim Park. Analysis results showed that the replanting activities occurred in the mud flat of the western coasts by nature and people while in the eastern coast the erosion has happened. This was also demonstrated by the results of study on changes of coastline recently (Hieu et al., 2000). Besides restoring mangrove, the purpose of replanting was also the expansion of land use into the west sea. The replanting occurred after the deposition of sediment and the shallow seabed.

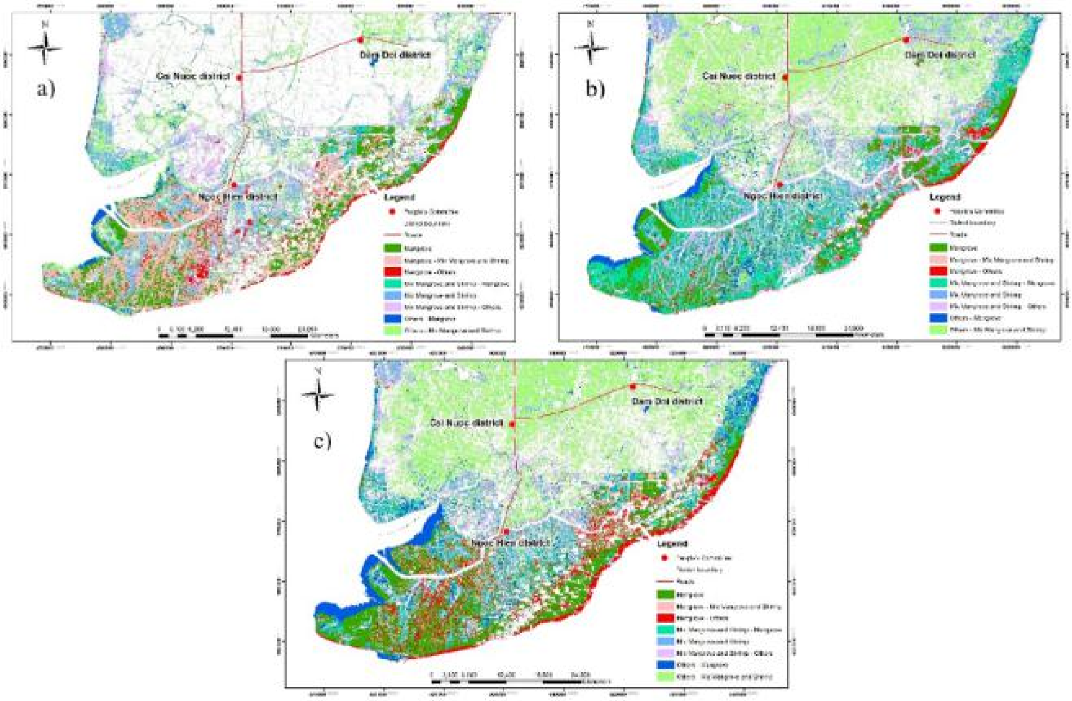

Fig. 7. Changes in mangrove forests in the study area from 1989 to 2015. a) Changes in 1989-1998, b) changes in 1998-2015, and c) changes in 1989-2015.

From above analysis, although some areas of mangrove were replanted, mangrove in study areas have been decreasing both in quantity and quality. There are many factors, which degraded mangrove, but the major one was shrimp culture activities. Other factors such as transformation, industry, urbanization, degradation of environment and sedimentation also impacted mangrove changes. These factors also had relationship with one another. On the contradictory, shrimp culture, on one hand, supplied nutrient salts for mangrove based on water and sediment discharge into mangrove areas. On the other hand, farmers have cut down mangrove and conversed to shrimp farms. Further, because of lack of information on environmental conditions, shrimp culture techniques and financial resources, shrimp culture failed in some areas or shrimp ponds were only used in a short period (Hong, 1995). After few years, land has been degraded and farmers continued to cut down mangrove to make new shrimp ponds.

The attitude of mangrove destruction and degradation was based on short-term exploitation for immediate economic benefit, rather than longer-term but sustainable exploitation. These are major causes of mangrove deforestation in the period of 1989 – 1998. However, human activities impact mangrove forests. Transportation increased suspended sediment. Agriculture also increased soil acidification and agrochemical in water but agricultural production has low values (Hong and San, 1993). These chemicals impacted negatively on shrimp farms and mangrove forests (Hong, 1995). In addition, other demand activities also caused conflicts of natural resources users and then affected mangrove forests. Beside of shrimp culture, huge areas of mangrove forests have been lost due to wood extraction, conversion to agriculture or salt production, coastal industrialization and urbanization and the war, but these areas have been equaled to mangrove forest areas where shrimp farming has been blamed for large scale losses.

4. CONCLUSIONS

This research successfully applied a new method to created cloud free Landsat data by using a histogram matching model and modified NSPI approach. In addition, mangrove forests was extracted based on characteristics, singularities, and distribution as well as reflectance values and spectral properties of mangrove forest in the images. The classification results indicated satisfactory agreement with the ground reference data with overall accuracy of

77.4% and Kappa coefficient of 0.68. After 26 years, mangrove forest lost more than 9% of the total area due to land use conservation and coastal erosion, but more than half of mangrove forest, which has existed, was low density. In addition, mangrove was recovered or newly planted by 277.4km2 (11.3%) at the same time.

These changes of mangrove forests were affected by two activities: deforestation and replanting but capacity of planting. The major reason of recent mangrove changes was shrimp farm development. Shrimp farm development and degradation also caused environmental and natural resource problem as well as socio-economic aspects. Reforestation of ineffective shrimp ponds might be a good solution to improve the sustainability of this ecosystem before one can make a master plan of land uses for the coastal zone to help solve these problems.

REFERENCES

Hong, P. N., and San, H. T., 1993. Mangrove of Vietnam, IUCN, 173pp.

Hong, P. N., 1995. Impact of shrimp culture extension on environment and biodiversity resources in marsh of coastal zone). Journal of Fisheries, No 3/1995. p. 6-9 and 25.

Hao, N. V., 1999. Shrimp Health Research in Vietnam, Including Current and Planned Activities. In "Towards Sustainable Shrimp Culture in Thailand and the Region". Ed. Paul T. Smith. Proceedings of a workshop, Hat Yai, Songkhla, Thailand, 28 Oct. – 1 Nov. 1996. p. 94-97.

Blasco,F., Carayon, J. L., and Aizpuru M., 2001. World Mangrove Resources, Glomis Electronic Journal.

Everitt, J. H., Yang, C., Sriharan, S., and Judd, F. W., 2008. Using high resolution satellite imagery to map black mangrove on the Texas Gulf Coast, Journal of Coastal Research, 24, 1582-1586.

Giri, C., Pengra, B., Zhu, Z., Singh, A., and Tieszen, L. L., 2007. Monitoring mangrove forest dynamics of the Sundarbans in Bangladesh and India using multi-temporal satellite data from 1973 to 2000. Journal of Estuarine, Coastal and Shelf Science, 73, 91-100.

Green,E. P., Mumby, P. J., Edwards, A. J., Clark, C. D. and Ellis A. C., 1998 The assessment of mangrove areas using high resolution multispectral airborne imagery, Journal of Coastal Resource, 14, 433-443.

Seto, K. C., and Fragkias, M., 2007. Mangrove conversion and aquaculture development in Vietnam: A remote sensing-based approach for evaluating the Ramsar Convention on Wetland, Journal of Global Environment Change, 17, 486-500.

Vaiphasa, C., Skidmore, A. K., and de Boer, W. F., 2006. A post-classifier for mangrove mapping using ecological data, ISPRS Journal of Photogrammetry and Remote Sensing, 61, 1-10.

Giri, E., Ochieng, L. L., Tieszen, Z., Zhu, A., and Singh T., 2011. Global Ecology and Biogeography, Global Ecology and Biogeography, 20, 154–159.

Berlanga, R., and Ruiz L., 2002. Land use mapping and change detection in the coastal zone of northwest Mexico using remote sensing techniques, Journal of Coastal Research, 18, 514-522.

Concheddaa, G., Durieuxb, L., and Mayauxa P., 2008. An object-based method for mapping and change analysis in mangrove system, ISPRS Journal of Photogrammetry & Remote Sensing, 63, 578-589.

Selvam, V., Ravichandran, K. K., Gnanappazham, L., and Navamuniyammal, M., 2003. Assessment of community-based restoration of Pichavaram mangrove wetland using remote sensing data, International Journal of Current Science, 85, 794-798.

Chen, C. F., Nguyen, T. S., Chang, N. B., Chen, C. R., Chang, L. Y., Valdez, M., Centeno, G., Thompson, C. A., and Aceituno J. L., 2013. Multi-Decadal Mangrove Forest Change Detection and Prediction in Honduras, Central America, with Landsat Imagery and a Markov Chain Model, Journal of Remote Sensing, 5, 6408-6426.

Jacques, P., Jean-Louis M., and Nguyen, T. A., 2002. Shrimp farming sustainability in the Mekong Delta: Environmental and technical approaches, in Proc. Workshop Held in Travinh (Vietnam), Tra Vinh, Vietnam, 54p.

GSO, 2012. Statistical Yearbook of Vietnam. Hanoi, Vietnam: General Statistics Office of Vietnam.

VNEPA, 2005. Overview of Wetlands Status in Viet Nam Following 15 Years of Ramsar Convention Implementation, Hanoi, Vietnam: Viet Nam Environment Protection Agency.

Chen, J., Zhu, X., Vogelmann, J. E., Gao, F., and Jin S., 2011. A simple and effective method for filling gaps in Landsat ETM+ SLC-off images, Remote Sens. Environ., 115, 4, pp. 1053–1064.

Eastman J. R., 1995. IDRISI for Windows, Version 1.0, Worcester MA: Clark University.

Swain, P. H., and Wacker A. G., 1971. Comparison of the Divergence and B-Distance in Feature Selection, Laboratory for the Applications of remote Sensing, Purdue University, West Lafayette, 12.

Jensen, J. R., 1996. Introductory Digital Image Processing: A Remote Sensing Perspective, 2nd ed. Upper Saddle River, NJ: Prentice Hall.

Huang, C., and Davis L. S., 2002. An assessment of support vector machines for land cover classification, International Journal of Remote Sensing, 23, 725–749.

Castro, E. A. and D. L., Donoho 2009. Does Median Filtering Truly Preserve Edges Better than Linear Filtering?, The Annals of Statistics 37, no. 3, 1172-1206.

Landis, J. R., and Koch, G. G., 1977. The measurement of observer agreement for categorical data, Biometrics, 159-174.
Hieu, T. T., Tiep, D. M., Trung, P. B. and Suu N. H., 2000. Status of the shore area from Tiengiang to Camau: causes of accumulation and erosion. Collection of Marine Research Works 10. p. 45-54.